Bull. Mater. Sci., Vol. 38, No. 2, April 2015, pp. 309–317. © Indian Academy of Sciences.

Effect of carbon nanofibre addition on the mechanical properties of different V_f carbon-epoxy composites

I SRIKANTH[1,2,*], SURESH KUMAR[2], VAJINDER SINGH[3], B RANGABABU[2], PARTHA GHOSAL[3] and Ch SUBRAHMANYAM[4]

[1]Department of Materials Science & Engineering, Indian Institute of Technology, Hyderabad 502 205, India
[2]Advanced Systems Laboratory, DRDO, Hyderabad 500 058, India
[3]Defence Metallurgical Research Laboratory, DRDO, Hyderabad 500 058, India
[4]Department of Chemistry, Indian Institute of Technology, Hyderabad 502 205, India

MS received 7 December 2013; revised 31 May 2014

Abstract. **Carbon-epoxy (C-epoxy) laminated composites having different fibre volume fractions (40, 50, 60 and 70) were fabricated with and without the addition of aminofunctionalized carbon nanofibres (A-CNF). Flexural strength, interlaminar shear strength (ILSS) and tensile strength of the composite laminates were determined. It was observed that, the ability of A-CNF to enhance the mechanical properties of C-epoxy diminished significantly as the fibre volume fraction (V_f) of the C-epoxy increased from 40 to 60. At 70V_f, the mechanical properties of the A-CNF reinforced C-epoxy were found to be lower compared to the C-epoxy composite made without the addition of A-CNF. In this paper suitable mechanisms for the observed trends are proposed on the basis of the fracture modes of the composite.**

Keywords. **Carbon-epoxy composite laminates; fibre volume fraction; carbon nanofibre; mechanical properties; delamination.**

1. Introduction

Owing to the good mechanical properties of the carbon nanofibres (CNFs), they are widely explored as an additional reinforcement to enhance the mechanical properties of the carbon fibre reinforced plastics (CFRPs).[1] Studies on generating required surface functional groups on CNF surfaces and dispersing them homogeneously in polymer matrices were reported extensively by many research groups which enables to realize full potential of CNF as reinforcements in CFRPs.[2–4] It is reported that, aminofunctional groups present on CNF can react with epoxy matrix and thus form a good bond with the matrix.[5] In general, improvement in the mechanical properties of CFRPs due to the addition of functionalized CNF is attributed to the strengthened fibre–matrix interface.[6] However, fibre volume fraction (V_f) of the composite has a strong effect on the fibre–matrix interface area. Hence, the extent of the mechanical properties improvement due to the CNF addition in CFRPs depends on the V_f of the composite.[7] This could be one of the reasons for the large scatter observed in the reported mechanical properties of CNF reinforced CFRPs. For instance, flexural strength improvements of fibre reinforced composite laminates due to the addition of CNF is reported upto as high as 22%, and also as low as 2.7%.[8,9] So far, it has not been established that, how CNF addition influences the mechanical properties of the CFRPs/C-epoxy composite laminates having different fibre volume fractions. The present study is aimed to bridge this gap. V_f of the composite used in most of the practical applications generally lies in the range of 40–70%. Therefore in this study, only this range is considered.

2. Experimental

8H Satin, T-300 carbon fabric (C-fabric) was used as reinforcement. Bisphenol-A-based epoxy with diethyl toluene diamine (DETDA) hardener was used as matrix. Aminofunctionalized carbon nanofibres procured from M/s Chemapal Industries (Mumbai, India) of diameter 100–150 nm (figure 1a and b) were used as an additional reinforcement.

For fabricating the composite laminates, initially 1.0 weight percentage (wt%) of A-CNFs (1.0 g of A-CNFs for 100 g of epoxy) were dispersed in the epoxy resin using a probe type ultrasonicator (Mesonix-3000, USA) for 45 min followed by ball milling at 250 rpm for 120 min. Hardener was added to the A-CNF–epoxy mixture (24 parts of hardener to 100 parts of the epoxy resin by weight). The mixture was further ball milled at 250 rpm for 30 min. C-fabric was cut into pre-decided specific dimensions and impregnated with A-CNF–epoxy–hardener mixture. Impregnated fabric layers were stacked and compressed in a suitable size metallic die. Curing of the stack in the compressed condition was carried out at 120°C for 120 min followed by 180°C for

*Author for correspondence (i_srikanth@yahoo.co.uk)

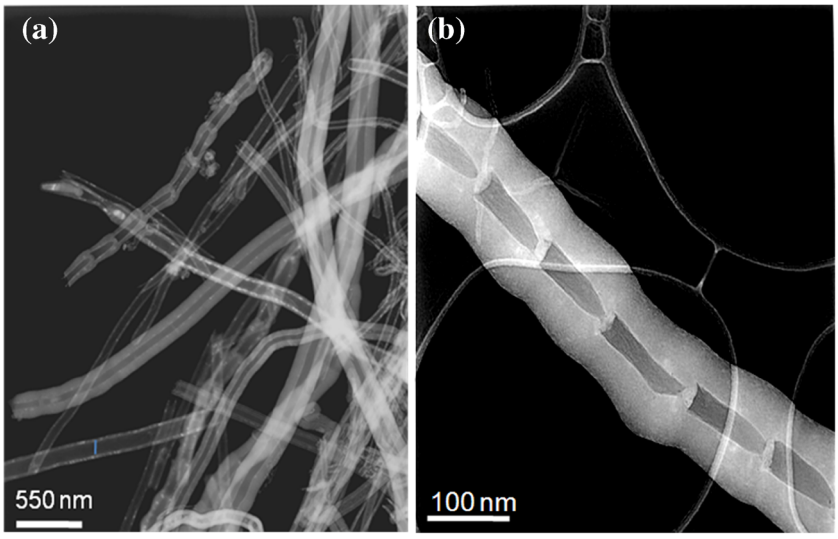

Figure 1. Morphology of as-received A-CNF as observed under transmission electron microscope at different magnifications.

Table 1. Details of C-epoxy composites fabricated.

Sample description	Sample code	wt% A-CNFs	V_f (±1)
Blank C-epoxy	40BCE	0	40
A-CNF–C-epoxy	40CCE	1.0	40
Blank C-epoxy	50BCE	0	50
A-CNF–C-epoxy	50CCE	1.0	50
Blank-C-epoxy	60BCE	0	60
A-CNF–C-epoxy	60CCE	1.0	60
Blank-C-epoxy	70BCE	0	70
A-CNF–C-epoxy	70CCE	1.0	70

180 min. V_f of the fabricated composite laminates was controlled by varying the number of fabric layers in the given thickness (approximately 2.5 mm). Different composite laminates that were made with varying V_f are as shown in table 1. Composite laminates made without A-CNF addition are denoted as BCE (Blank–carbon-epoxy) while the composite laminates made with the addition of A-CNF are denoted as CCE (CNF reinforced carbon-epoxy). The numbers prefixing the BCE/CCE indicate the fibre volume fraction. For instance, 60CCE indicates A-CNF reinforced C-epoxy composite having $60V_f$. Volume fraction of the composite laminates was determined with acid digestion test using concentrated nitric acid as per ASTM D3171. Flexural strength, interlaminar shear strength (ILSS) and tensile strength of the prepared composite laminates were determined as per ASTM D790 (three point bending test), ASTM D2344 and ASTM D638, respectively, on the universal testing machine (United 50KN, USA). Minimum eight numbers of samples were tested from each laminate for each of the measured property and the results obtained are shown in table 2. Microstructure and fracture modes of the tested samples were analyzed with environmental scanning electron microscopy (ESEM-FEI Quanta 400, The Netherlands).

2.1 *Fitting of experimental data*

Although for all practical purposes the actual test results are used for designing aerospace grade load bearing structures, still it is desired to fit the experimental data into an appropriate mathematical equation in order to estimate the strength at any required volume fraction between 40% and 70%. Since the obtained strength data is showing a quadratic trend as a function of fibre volume fraction, the flexural strength, ILSS and tensile strength of BCE and CCE composites are represented in quadratic equations, with V_f as a variant.

Generalized second-degree quadriatic equation is shown below.

Absolute strength (S) in MPa at a given V_f:

$$S = a + bV_f + cV_f^2,$$

where 'a' is the constant and 'b', 'c' the coefficients of fibre volume fractions under study. 'S' is the absolute average strength value taken from table 2. Typical quadratic equations that were generated from flexural strength values of BCE samples having different fibre volume fractions namely 40, 50, 60 and $70V_f$ are shown below.

$$\text{For 40BCE: } 529 = a + 0.4b + (0.4)^2c.$$
$$\text{For 50BCE: } 601 = a + 0.5b + (0.5)^2c.$$
$$\text{For 60BCE: } 765 = a + 0.6b + (0.6)^2c.$$
$$\text{For 70BCE: } 921 = a + 0.7b + (0.7)^2c.$$

The absolute values of flexural strength (S) of BCE at each of the V_f is taken from table 2.

Above equations were solved numerically to find the values of the coefficients, i.e., 'b', 'c' and constant 'a'. Similarly quadratic equations were generated for ILSS and tensile properties also for both BCE and CCE samples from the values

Table 2. Summary of the mechanical properties of composites.

Sample V_f	F.S.[a] (MPa) BCE	F.S.[a] (MPa) CCE	% Imp[b]	ILSS (MPa) BCE	ILSS (MPa) CCE	% Imp	T.S.[c] (MPa) BCE	T.S.[c] (MPa) CCE	% Imp
40	529 (23)	682 (41)	28.9	32 (1.2)	41 (1.1)	28.1	722 (42)	775 (26)	7.3
50	601 (39)	690 (44)	14.8	35 (2.8)	40 (1.8)	14.2	756 (23)	777 (7.4)	2.7
60	765 (38)	788 (38)	3.0	47 (2.4)	48 (1.6)	2.1	855 (18)	896 (42)	4.7
70	921 (28)	869 (27)	−5.6	47 (4.5)	45 (3.2)	−4.4	915 (14)	854 (39)	−6.6

[a]Flexural strength.
[b]Percentage improvements.
[c]Tensile strength.
Note: Values in the parentheses indicate standard deviations.

Table 3. Values of the co-efficients of quadratic equations for flexural strength, ILSS and tensile strength.

Sample code	Flexural strength a	Flexural strength b	Flexural strength c	ILSS a	ILSS b	ILSS c	Tensile a	Tensile b	Tensile c
BCE	−0.9	1183.8	168.6	−0.078	87.8	−31.4	−0.9	2333.6	−1488.1
CCE	−1.4	2077.8	−1221.2	−0.097	140.6	−112.2	0.4	2865.8	−2306.6

Table 4. Comparison of the theoretically predicted values against experimentally obtained mechanical properties for 55CCE.

Sample code	F.S.[a] (MPa)	ILSS (MPa)	T.S.[b] (MPa)
55CCE			
Calculated	770	44	879
Experimental values	705 (29)	47.5 (1.6)	849 (21)
Dev[c]	8.4	7.9	3.4

[a]Flexural strength.
[b]Tensile strength.
[c]Percentage deviation.
Note: Values in the parentheses indicate standard deviations.

that were experimentally obtained. Resultant quadratic equations were solved. Obtained coefficients for quadratic equation for flexural, ILSS, tensile strength of BCE, CCE are shown in table 3. To validate the equations, C-epoxy composite having 55V_f is made with the addition of 1 wt% of A-CNF (55CCE). Correlation is made between the experimentally obtained values to the mathematically expected mechanical properties which are shown in table 4.

3. Results and discussion

3.1 *Flexural strength*

3.1a *Flexural strength at 40–60V_f*: A-CNF reinforced C-epoxy (CCE) composite laminates have shown higher flexural strength as compared to their corresponding blank (BCE) composite laminates having same V_f (table 2).

However, as the V_f of the composite increases, there is a visible downward trend in the percentage improvements of the flexural strength for CCE against their corresponding BCE (having same V_f). For instance, flexural strength of 40CCE is 28.9% higher than 40BCE, while it is only 3% higher for 60CCE as compared to 60BCE. SEM studies of the fractured specimens have shown good dispersion of A-CNF at all V_f (40–70%) of the composite laminates (figure 2). Hence, the observed variation of the flexural strength improvements as a function of V_f of the C-epoxy can be attributed to the reasons other than the A-CNF dispersion problems. As all other experimental parameters were kept same except variation of V_f while preparing composite, the systematic change in the degree of flexural strength improvements can be attributed to the effects of V_f only. The reasons for such a trend in the flexural strength imposed by V_f can be understood from the failure modes of the C-epoxy composites. Flexural failure of the composite is known to involve a combination of tensile failure of the reinforcements and interlaminar failure due to the shearing of the fibre–matrix interface. SEM images of the BCE and CCE failed under flexural loads, show failure by combination of these two modes with rupture of the fabric layers and shearing at the fibre–matrix interface (figure 3). It was observed that the magnitude of the former and latter modes of the failures varied significantly for BCE and CCE. For instance, in case of 40BCE, failure initiated under the loading point in the flexural strength test, resulted in the predominant formation of interlaminar cracks due to interface shearing (figure 3a). It is well reported that, the crack propagation through the matrix-rich interface zones encounters less resistance.[7] Hence, 40BCE failed at lower strength. On the other hand, in case of 40CCE, crack propagation was

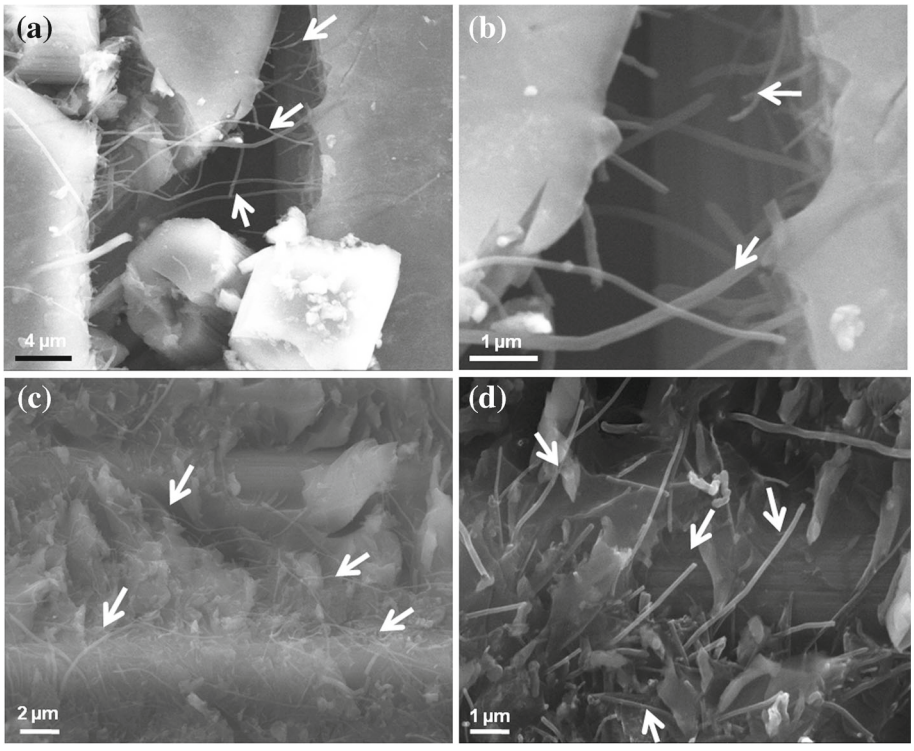

Figure 2. Fractured samples of C-epoxy composites failed under flexural/tensile loads showing good dispersion of A-CNF (indicated by arrows): (**a**) 40CCE failed under flexural load, (**b**) 50CCE failed under flexural load, (**c**) 40CCE failed under tensile load and (**d**) 60CCE failed under tensile load.

predominantly translaminar with the rupture of the C-fabric layers with minimum or no interface shearing (figure 3b). This mode of failure indicates that A-CNF strengthened the interface due to their ability to interlock the fibre–matrix interface as shown in figure 3c.[10,11] As the C-fibre rupture consumes more energy, failure through the translaminar crack propagation with the rupture of C-fibres, resulted in a significant improvement in the flexural strength for 40CCE. Schematic failure modes of BCE and CCE at low V_f are shown in figure 4a and b. Besides this, the epoxy matrix, reinforced by the A-CNF is known to exhibit enhanced stiffness. Stiffened matrix can effectively restrain fibre bending which also contributed to the improved flexural strength of 40CCE.[12–14]

As the V_f of the composite laminates increased to $60V_f$, the fracture modes have changed significantly. In case of both 60BCE and 60CCE crack propagation mode during flexural failure was observed to be predominantly translaminar (figure 3d and e). Reduced interface shearing even for BCE at higher V_f can be attributed to the crimp of the woven fabrics which is a curvature or deformation arising out of weaving.[15] At higher V_f, when the adjacent fabric layers are well compacted, crimp zones can interlock with adjacent fabric layer zones having complementary curvatures. These interlocks could resist interface shearing. Thus, at the higher V_f of C-epoxy, crack propagation is proceeding with rupture of carbon fabric layers even for BCE samples. Hence, need of A-CNF to resist the interlaminar cracks would be limited for higher V_f C-epoxy composites. Thus, as both, 60BCE and 60CCE failed in a similar mode, a significant improvement in the flexural strength due to the addition of A-CNF was not observed. Schematic failure of the 60BCE (high V_f C-epoxy) is shown in figure 4c.

Marginal improvement in the flexural strength for 60CCE as compared to 60BCE, even at $60V_f$ can be attributed to A-CNF present in CCE, which can still offer improved matrix stiffness. This results in enhanced resistance to the C-fibre bending and thus enhanced flexural strength.

3.1b *Flexural strength at $70V_f$*: Addition of A-CNFs to the C-epoxy laminates having $70V_f$ (70CCE) was found to reduce the flexural strength (table 2) by 6.6% as compared to 70BCE. Failure of the 70CCE involved a mixed mode of failure with rupture of the C-fabric coupled with the interlaminar failure (figure 3f and g). Unlike in 40CCE, where A-CNF could arrest interlayer cracks, in case of 70CCE, they could not arrest the interlayer/laminar crack propagation. This could be attributed to poor wetting of the C-fibres in 70CCE. When, A-CNFs are present in the composite, they compete with the C-fibres in consuming the resin for wetting their surfaces. Hence, at such higher V_f, the epoxy resin may not be sufficient to achieve ideal wetting of C-fibres. This can

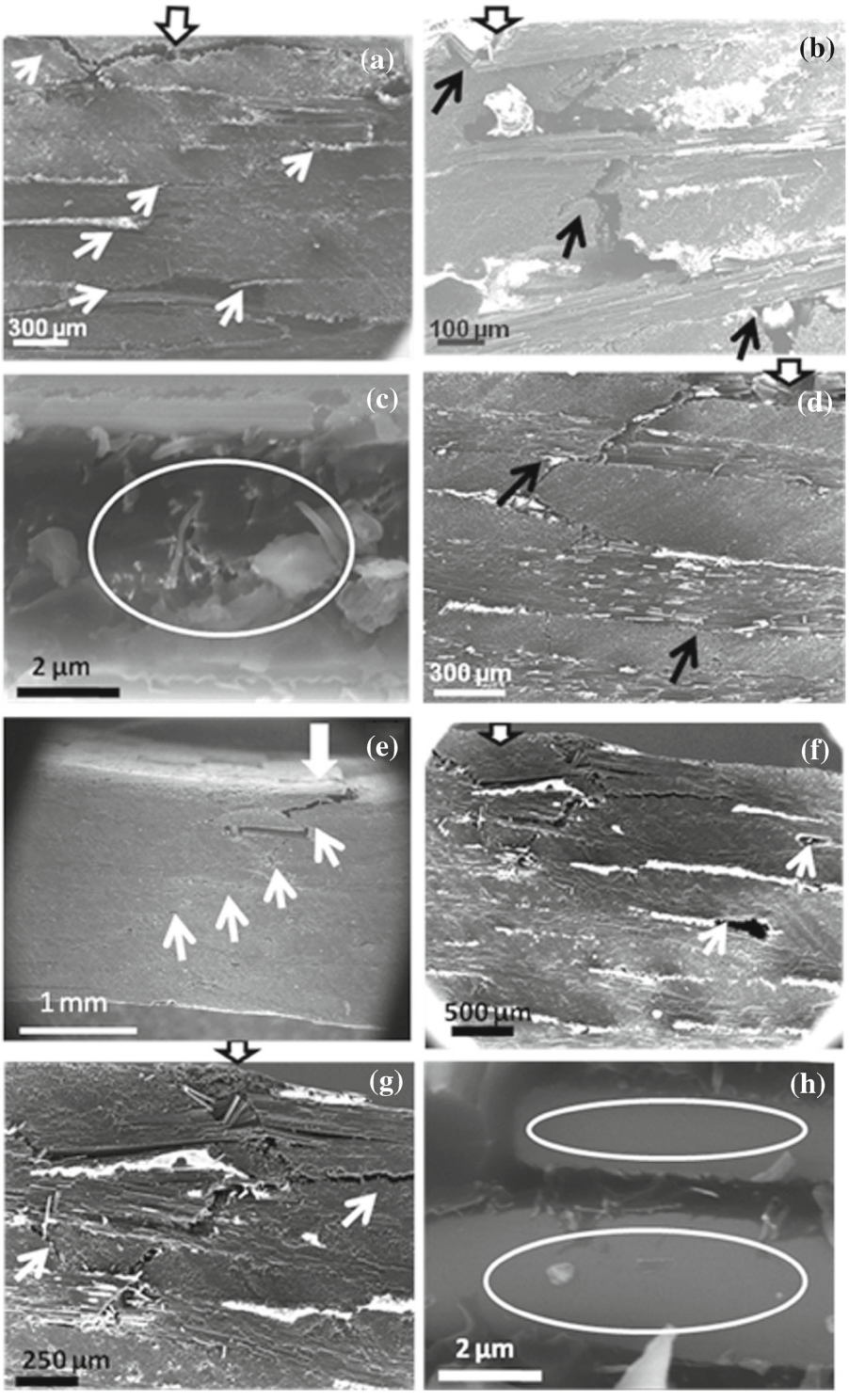

Figure 3. Showing C-epoxy samples failed under flexural loads. Broad arrows on top of each figure are indicating the loading point: (**a**) 40BCE showing failure predominantly by interlaminar crack propagation (indicated by arrows), (**b**) 40CCE showing predominant failure by rupture of C-fabrics (indicated by arrows) with no interlaminar crack propagation, (**c**) SEM image of 40CCE showing interface strengthening by A-CNF (encircled zone), (**d**) 60BCE and (**e**) 60CCE showing failure by rupture of C-fabric layers with minimum interlaminar crack propagation (crack propogation path identified with arrows), **f** and **g** showing mixed mode of failure of 70CCE sample with significant interlaminar crack propagation (indicated by arrows) coupled with rupture of carbon fabrics and (**h**) encircled zones showing matrix removal from the surface of the C-fibres indicating poor wetting for 70CCE.

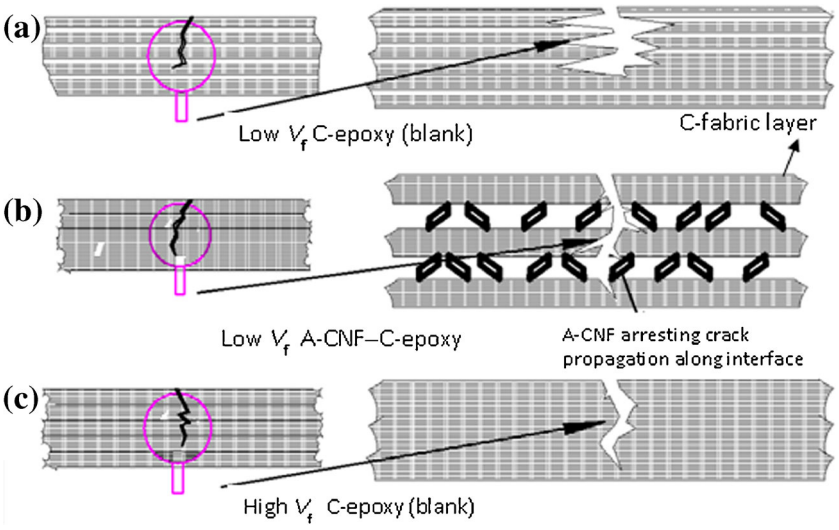

Figure 4. Showing schematic flexural failure modes of C-epoxy/A-CNF–C-epoxy with different V_f: (**a**) low V_f C-epoxy showing horizontal spread of crack at each layer giving more interlaminar crack propagation, (**b**) low V_f C-epoxy with A-CNF showing, A-CNF arresting the horizontal spread of crack and forcing the crack to propagate by rupturing C-fabric layers and (**c**) high V_f C-epoxy showing highly compacted C-fabric layers and translaminar crack propagation.

be evidenced from the poor wetting of the C-fibres in 70CCE (figure 3h) as compared to the wetting for 40CCE (figure 3c). This is due to the fact that, carbon nanofibres which are having significantly high surface area would have consumed considerable proportion of the available resin. Resin insufficiency to ensure ideal bonding between fibre–matrix, lead to generation of a weak interface along which crack propagated in a facile manner leading to reduction in the flexural strength. In case of 70BCE, there were no A-CNFs to compete for the resin with the C-fibres. Due to good wetting of C-fibres, as well as the effective interlocking of alternate fabric layers with crimp zones of the fabrics, 70BCE has shown better flexural strength as compared to 70CCE.

3.2 *Tensile strength*

Visible improvement in tensile strength due to the A-CNF addition was observed for C-epoxy (table 2). Reasons for this can be understood from the fracture modes of the BCE and CCE samples. Figure 5 shows that the tensile failure of the C-epoxy involved interfilament debonding at the microlevel and interlayer debonding at the macrolevel. However, the magnitude of the interfibre and interlayer debonding varied significantly from BCE to CCE. Reasons for these observations are discussed below.

3.2a *Interfibre debonding*: It is observed that the fracture surfaces of the BCE were smooth with complete interfilament debonding (figure 5a), while CCE have shown strong interfilament bonding due to the fibre–matrix interface locking by A-CNF (figure 5b). SEM images also show that there is significant toughening at the fibre–matrix interface as inferred from the rough surfaces that were observed on the fractured surfaces (figure 5c). This could be due to the fact that, aminofunctional groups present on the surface of the CNFs, can participate in the crosslinking reaction with the epoxy matrix resulting in enhanced interface crosslink density. The increased crosslink density at the interface results in an enhanced interface toughness.[16] Besides this, A-CNFs introduced in CFRPs preferentially assumed the interface position of C-filament to matrix due to filtration effects of C-filaments (figure 5b and c). These, A-CNFs which are present at the interface can enhance the interface strength and thus cause, delayed interfibre crack initiation.[17] Schematic of the interfibre/filament bond strengthening by A-CNF in CCE is shown in figure 6a and schematic of poor interfilament bonding in BCE is shown in figure 6b. Enhanced interface toughness and enhanced bridging of interfaces due to A-CNF, can involve more number of reinforcing fibres/filaments during tensile failure of the composite.[18,19] Thus for CCE, higher interface toughness coupled with strong interfilament bonding ensured uniform load distribution across all the carbon fibres.[19,20] Hence, CCE samples have shown higher tensile strength.

3.2b *Interlayer bond strengthening*: When a composite is subjected to the external stress, a shear stress is generated between the reinforcement and matrix due to the elastic mismatch according to the shear lag theory.[21] Beyond a critical stress, interfacial slipping occurs which results into shearing at the fibre–matrix interface. This leads to generation of the interlayer cracks and debonding of layers. This could result in non-uniform load distribution across the sample leading to premature failure of the composite. This can be

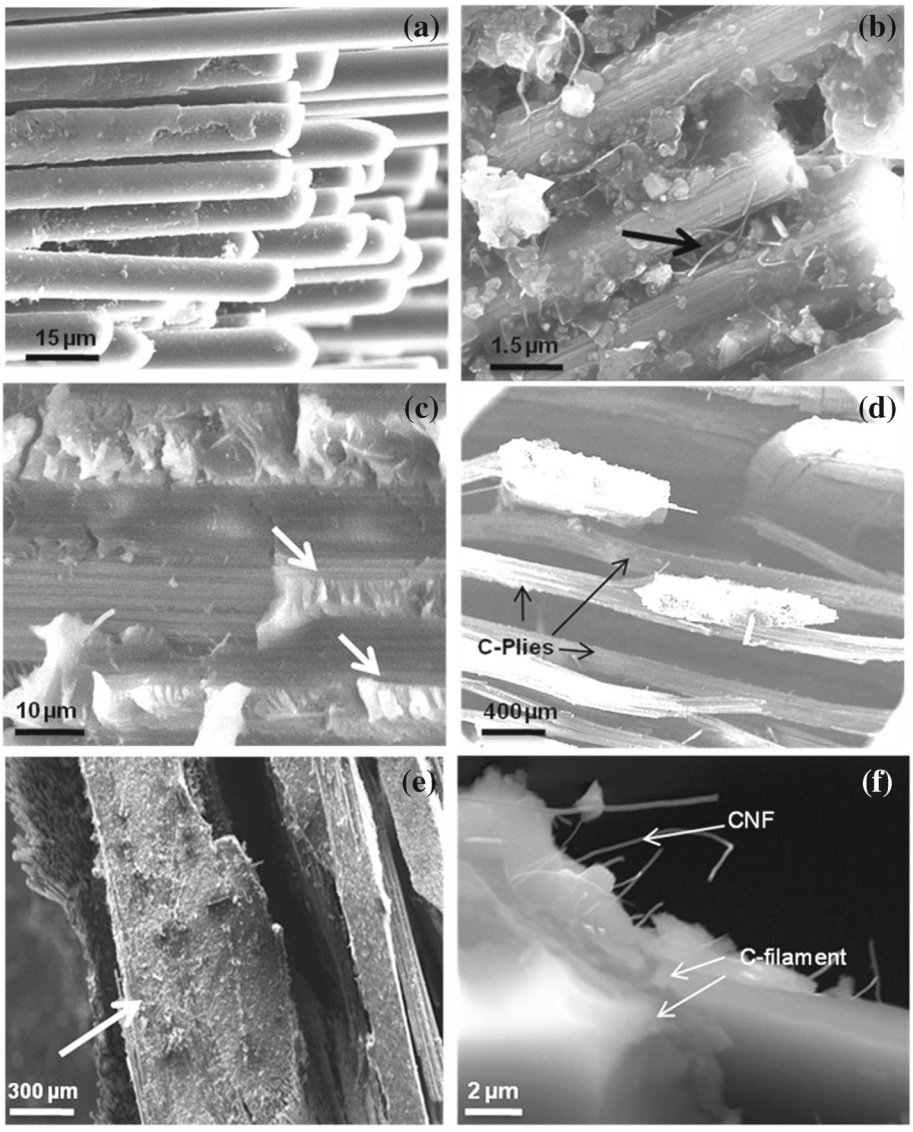

Figure 5. SEM images of C-epoxy samples failed under tensile loads: (**a**) 40BCE showing interfilament debonding, (**b**) 40CCE showing strong interfilament bonding due interlocking of filaments by A-CNF (indicated by arrow), (**c**) 60CCE showing rough surface with hackle like features, indicating interface toughening (indicated by arrows), (**d**) 60BCE showing interlayer (plies) delamination during tensile failure, (**e**) 60CCE showing improved interply bonding (shown by arrow) up to ultimate tensile strength and (**f**) 60CCE showing A-CNF projections from C-filaments from the fracture zones.

evidenced from the SEM images of BCE, which has shown significant interlayer delamination during the tensile failure (figure 5d). However, for CCE, interlayer delamination has come down drastically (figure 5e). This is due to locking of C-fibres to the matrix at the interface, which minimized the differential strains at the fibre–matrix interface. Besides this, long projections of A-CNFs from the C-fibre surfaces as shown in figure 5f, indicates possible Z-reinforcement of the various layers which can further minimize the interlayer debonding.[7,12,13] Schematic of the interlayer strengthening of CCE due to Z-reinforcement of A-CNF is shown in figure 6c and poor interlayer bond strength of BCE is shown in figure 6d.

Thus, the strengthened fibre–matrix bonding at the microlevel and interlayer bonding at the macrolevel lead to a uniform load distribution across the sample under tensile load. This resulted in a higher tensile strength for CCE samples.

Similar to the trend that was observed for flexural properties, the tensile strength of 70CCE was observed to be lower as compared to 70BCE. Fracture mode of the 70CCE was observed to be predominantly with interlayer debonding as shown in figure 7a. As explained previously, A-CNF addition to $70V_f$ C-epoxy has led to the resin insufficiency and thus inefficient wetting of the C-fibre surface as shown in figure 7b. This inturn resulted in the generation of the interfacial cracks and thus facile interfilament (figure 7c) and

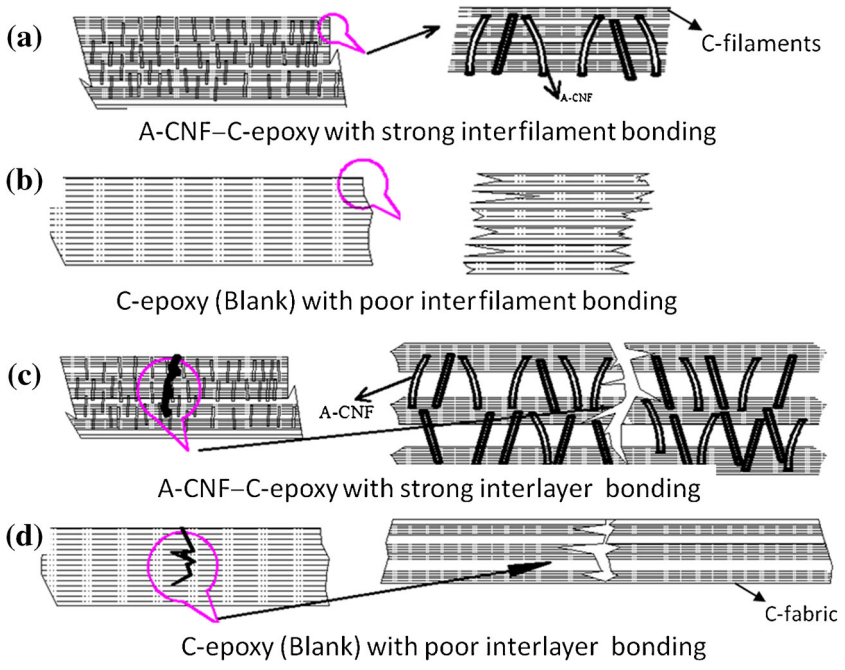

Figure 6. Showing schematic tensile failure modes of C-epoxy with and without A-CNF: (**a**) interfilament bond strengthening by A-CNF there by involving more C-filaments/fibres during failure, (**b**) C-epoxy without A-CNF showing poor interfilament bonding, (**c**) C-epoxy with A-CNF showing interply bonding due to Z-reinforcement of by A-CNF and (**d**) C-epoxy without A-CNF showing more interply debonding.

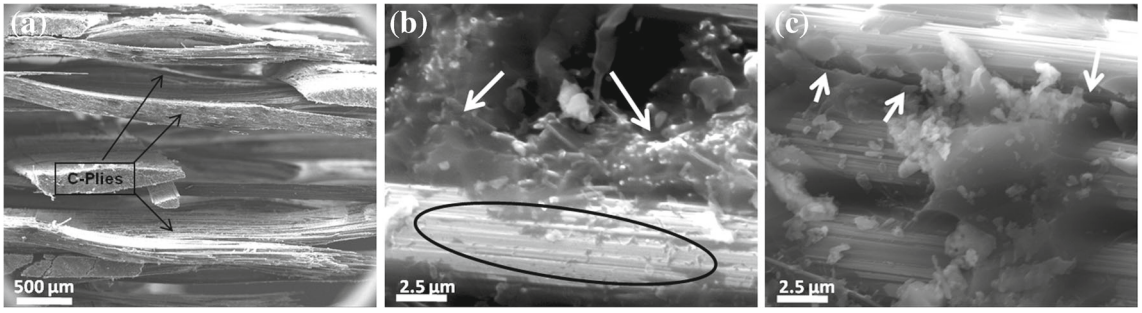

Figure 7. 70CCE samples failed under tensile load: (**a**) significant interply debonding during tensile failure, (**b**) encircled zone showing poor bonding of the C-fibres with matrix, and preferential matrix attachment with A-CNF at interface (shown by arrows) and (**c**) crack initiation at the fibre matrix interface (shown by arrows).

interlayer debonding (figure 7a). Hence, the tensile strength of the 70CCE was lower than 70BCE.

3.3 *ILSS*

ILSS of the CCE samples are higher as compared to the BCE. However, percentage improvements in ILSS have come down as the V_f increased (table 2). For instance, for 40CCE, ILSS was 28.1% higher as compared to the 40BCE while it was only 2.1% higher for 60CCE as compared to 60BCE. A-CNF addition should result in more ILSS because CNFs provide more interfacial surface area and also act as interlocks at the fibre–matrix interface which effectively resists interface shearing.[6] Decrease in the percentage improvement of ILSS with the increase in V_f of the composite can be attributed to the enhanced fibre surface area in the high V_f composite laminates, which needs to be bridged/anchored with the matrix. As the amount of A-CNFs in C-epoxy composite laminates of different fibre volume fractions was kept same in the present study, the effectiveness of the A-CNFs in arresting the interface shearing has come down with the increase in fibre volume fraction or fibre/matrix interface area. 70CCE has shown lower ILSS than 70BCE (table 2), because of matrix insufficiency observed at this V_f to form ideal bonding with both carbon fibres and A-CNFs.

3.4 *Validation of mathematical model*

The co-efficients of the equations that were generated for BCE and CCE for flexural, ILSS and tensile properties are shown in table 3.

The fitment of above coefficient, with respect to the values reported in table 2 are observed to be very close with minimum and maximum deviations of 0.5% and 7% in case of flexural strength, 2.1% and 12% in case of ILSS and 0.3% and 10.1% in case of tensile strength.

Experimentally obtained mechanical properties of the $55V_f$ A-CNF–C-epoxy composite are shown in table 4. Theoretically predicted mechanical properties using the coefficients shown in table 3 in proposed quadratic equations are also in table 4. It can be seen that the, experimentally obtained mechanical properties of the CCE having $55V_f$, are matching closely with the predicted mechanical properties with a maximum deviation of around 8%.

4. Conclusions

(i) With the procedure adopted in the present study aminofunctionalized carbon nanofibres (A-CNF) upto 1% by epoxy matrix weight can be dispersed satisfactorily.

(ii) A-CNF can impart significant enhancement in the flexural, shear and tensile strength of the laminated carbon–epoxy composite laminates having lower fibre volume fractions (around 40%). However, as the fibre volume fraction of the composite increased (around 60%), strengthening mechanisms due to A-CNF are losing their prominence and thus giving only marginal improvement in the above properties.

(iii) Addition of A-CNF to C-epoxy composite laminates having very high fibre volume fraction (70% fibre volume fraction in present study) results in reduction in mechanical properties due to inability of the available matrix to form ideal bond with both A-CNF and C-fibres.

(iv) Addition of A-CNF would be beneficial for C-epoxy composites having fibre volume fractions in the range of 40–60%, while beyond 60% V_f , they may degrade the mechanical properties.

(v) From the actual mechanical properties that were obtained for blank C-epoxy and A-CNF–C-epoxy composites at different fibre volume fractions, simple mathematical models are proposed to estimate the mechanical properties C-epoxy composites having any unknown fibre volume between 40% and 70%. The model is validated with the experimental work and found to be working satisfactorily.

References

1. Tibbetts G G, Lake M L, Strong K L and Rice B P 2007 *Compos. Sci. Technol.* **67** 1709
2. Li J, Vergne M J, Mowles E D, Zhong W-H, Hercules D M and Lukehart C M 2005 *Carbon* **40** 2883
3. Prolongo S G, Camp M, Gude M R, Chaos-Moran R and Urena A 2009 *Compos. Sci. Technol.* **69** 349
4. Rana S, Alagirusamy R and Joshi M 2011 *Composites A* **42** 439
5. Shen J, Huang W, Wu L, Hu Y and Ye M 2007 *Compos. Sci. Technol.* **67** 3041
6. Green K J, Dean D R, Vaidya U K and Nyairo E 2009 *Composites A* **40** 1470
7. Wichmann M H G, Sumfleth J, Gojny F H, Quaresimin M, Fielder B and Schulte K 2006 *Eng. Fract. Mech.* **73** 2346
8. Zhou Y, Pervin F, Jeelani S and Mallick P K 2008 *J. Mater. Proc. Technol.* **198** 445
9. Iwahori Y, Ishiwata S, Sumizawa T and Ishikawa T 2005 *Composites A* **36** 1430
10. Wicks S S, De Villoria R G and Wardle B L 2010 *Compos. Sci. Technol.* **70** 20
11. Godara A, Mezzo L, Luizi F, Warrier A, Lomov S V, Van Vuure A W, Gorbatick L, Moldenaers P and Verpoest I 2009 *Carbon* **47** 2914
12. Gojny F H, Wichmann M G, Fiedler B, Bauhofer W and Schulte K 2005 *Composites A* **36** 1525
13. Gojny F H, Wichmann M H G, Kopke U, Fiedler B and Schulte K 2004 *Compos. Sci. Technol.* **64** 2363
14. Tomohiro Y, Iwahori Y, Ishiwata S and Enomoto K 2007 *Composites A* **38** 2121
15. Savage G 1993 *Carbon–carbon composites* (London: Chapman & Hall) p. 68
16. Srikanth I, Kumar S, Kumar A, Ghosal P and Subrahmanyam Ch 2012 *Composites A* **43** 2083
17. Gorbatikh L, Lomov S V and Verpoest I 2011 *Proc. Eng.* **10** 3252
18. Tsantzalis S, Karapappas P, Vavouliotis A, Kostopoulos P, Tanimoto T and Friedrich K 2007 *Composites A* **38** 1159
19. Karapappas P, Vavouliotis A, Tsotra P, Kostopoulos V and Paipetis A 2009 *J. Compos. Mater.* **43** 977
20. Davis D C, Wilkerson J W, Zhu J and Hadjev V G 2011 *Compos. Sci. Technol.* **71** 1089
21. Khan S U, Li G Y, Siddiqui N A and Kim J K 2001 *Compos. Sci. Technol.* **71** 1486